Journal of Power Sources 196 (2011) 4785–4790

Contents lists available at ScienceDirect

Journal of Power Sources

journal homepage: www.elsevier.com/locate/jpowsour

Direct observation of the partial formation of a framework structure for Li-rich layered cathode material $Li[Ni_{0.17}Li_{0.2}Co_{0.07}Mn_{0.56}]O_2$ upon the first charge and discharge

Atsushi Ito [a], Kaoru Shoda [b], Yuichi Sato [c], Masaharu Hatano [a], Hideaki Horie [a], Yasuhiko Ohsawa [a,*]

[a] Nissan Research Center, Nissan Motor Co., Ltd., 1, Natsushima-cho, Yokosuka, Kanagawa 237-8523, Japan
[b] UBE Scientific Analysis Laboratory, Inc., Tokiwadai, Ube-shi, Yamaguchi 755-0001, Japan
[c] Department of Material and Life Chemistry, Faculty of Engineering, Kanagawa University, 3-27-1, Rokkakubashi, Kanagawa-ku, Yokohama 221-8686, Japan

ARTICLE INFO

Article history:
Received 27 September 2010
Received in revised form
11 December 2010
Accepted 21 December 2010
Available online 7 January 2011

Keywords:
Cathode material
$Li[Ni_{0.17}Li_{0.2}Co_{0.07}Mn_{0.56}]O_2$
HAADF-STEM

ABSTRACT

The structural changes upon the first charge and discharge of a Li-rich layered cathode material $Li[Ni_{0.17}Li_{0.2}Co_{0.07}Mn_{0.56}]O_2$ were investigated using high-angle annular dark-field scanning transmission electron microscopy (HAADF-STEM) and selected-area electron diffraction (SAED). Atomic resolution STEM observations revealed that some of the transition metal (TM) atoms were transferred from the TM layers to the Li layers upon the first charge and discharge, leading to the partial formation of a framework structure. This framework structure was considered as a spinel structure based on our simulation results of the corresponding SAED pattern of the fully charged state. This framework structure was also recognized even at the early stage of the first charging process in the plateau region around 4.5 V by using the SAED patterns, indicating that the formation of this framework structure started at the same time as the electrochemical activation.

1. Introduction

High performance Li-ion batteries have been indispensable as a key component of the smart grid electricity network systems used to overcome the global warming problem. To increase the specific energy of Li-ion batteries, it is necessary to increase the capacity of the cathode because the usable capacity of graphite as an anode, about 350 mAh g^{-1}, is much larger than that of $LiCoO_2$ as a cathode (150 mAh g^{-1}) [1], a material that is widely used as the cathode in Li-ion batteries. Therefore, numerous cathode materials have been investigated to increase the specific energy of Li-ion batteries.

It has been reported that the Li-rich solid-solution layered cathode material Li_2MnO_3–$LiMO_2$ (M = Co, Ni, etc.) exhibits a capacity greater than 200 mAh g^{-1} when operated above 4.6 V, making it a promising candidate for the cathode material [2]. However, the mechanism of the charge–discharge reaction has not yet been clarified [3–6]. To clarify this mechanism, we have analyzed the local structure of the as-prepared $Li[Ni_{0.17}Li_{0.2}Co_{0.07}Mn_{0.56}]O_2$ ($0.4(Li_2MnO_3)$–$0.4(LiMO_2)$, $M = Ni_{0.425}Co_{0.175}Mn_{0.4}$) cathode material as a typical example using high-angle annular dark-field scanning transmission electron microscopy (HAADF-STEM) and X-ray absorption spectroscopy (XAS) [7], and we have examined the changes in the valence states of transition metal (TM) atoms for this cathode material during the charge–discharge using *in situ* XAS [8].

In this study, the structural changes of the $Li[Ni_{0.17}Li_{0.2}Co_{0.07}Mn_{0.56}]O_2$ upon the first charge and discharge were examined using HAADF-STEM and selected-area electron diffraction (SAED). It was clearly showed that Li ions were located in a periodic pattern at the TM layers of the as-prepared cathode material. We observed that the periodicity collapsed during the first full charge process, and that some measures of this periodicity returned during the first discharge process. We found that some of the TM atoms were transferred from the TM layers to the Li layers during the first charge and discharge processes, partly forming a framework structure, probably a spinel structure.

2. Experimental

$Li[Ni_{0.17}Li_{0.2}Co_{0.07}Mn_{0.56}]O_2$ cathode material was prepared using a coprecipitation method and was characterized using inductive-coupled plasma spectroscopy and X-ray diffraction, as detailed elsewhere [2,9]. To obtain charged and discharged cathode materials, coin-type cells were made [9]. After charge and discharge, the cells were disassembled in a glove box and the cathodes were washed with dimethyl carbonate (DMC) several times, followed by drying in a vacuum. TEM specimens were prepared from the cathodes. The sample particles that were scrapped off from

* Corresponding author. Tel.: +81 46 867 5367; fax: +81 46 865 5796.
E-mail address: y-oosawa@mail.nissan.co.jp (Y. Ohsawa).

0378-7753/$ – see front matter © 2011 Elsevier B.V. All rights reserved.
doi:10.1016/j.jpowsour.2010.12.079

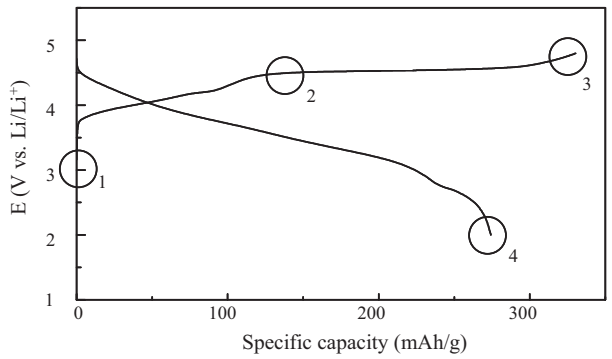

Fig. 1. The first charge and discharge curves of the $Li[Ni_{0.17}Li_{0.2}Co_{0.07}Mn_{0.56}]O_2$ cell. The test was performed at a constant current density of 0.2 mA cm^{-2} between 2.0 and 4.8 V at room temperature. TEM experiments were performed at stages 1, 2, 3 and 4 in the curves, corresponding to the as-prepared, plateau region at 4.5 V, fully charged at 4.8 V, and fully discharged at 2.0 V states, respectively.

the cathodes were embedded in epoxy resin and thinned by hand lapping, followed by Ar ion milling.

SAED patterns were acquired with a JEOL JEM-2010F field emission (FE) TEM operated at 200 kV. HAADF-STEM observation was carried out with a JEOL JEM-ARM200F FE-TEM operated at 200 kV equipped with a STEM Cs corrector, which provided a STEM resolution of less than 0.1 nm. HAADF-STEM images were analyzed by a fast Fourier transform technique, which also reduced the noise of the images. To estimate the TM composition from the images, the image contrast intensity was calculated with a multislice simulation program (HREM Research Inc.) [10].

3. Results and discussion

Fig. 1 shows the first charge and discharge curves for a coin cell made with the $Li[Ni_{0.17}Li_{0.2}Co_{0.07}Mn_{0.56}]O_2$ cathode material, where the charge and discharge processes were performed in the potential range of 2.0–4.8 V (vs. Li^+/Li) at a constant current of 0.2 mA cm^{-2}. The charge curve shows that the cell had a plateau region at 4.5 V and was fully charged at 4.8 V with a capacity of more than 300 mAh g^{-1}. To clarify the structural changes, we focused on the material in its as-prepared, fully charged (4.8 V) and fully discharged (2.0 V) states, as denoted by stages 1, 3 and 4 in the curves, respectively. We also investigated the plateau region at 4.5 V, as denoted by stage 2.

The crystal structure of $Li[Ni_{0.17}Li_{0.2}Co_{0.07}Mn_{0.56}]O_2$ is basically a layered α-$NaFeO_2$ type crystal with the Li atoms occupying the Na sites, and with the Li and TM atoms occupying the Fe sites. Fig. 2 shows the atomic resolution HAADF-STEM images for the as-prepared particle along the $[1\,0\,\bar{1}\,0]$ and $[1\,1\,\bar{2}\,0]$ zone axes, with the corresponding SAED patterns inserted in the images. Both images were taken from the same particle. Bright dots in the HAADF-STEM images correspond to the atomic columns, and Li atoms are invisible because the contrast of an atomic column in the HAADF-STEM image is almost proportional to the square of the atomic number (Z^2). The contrast of an atomic column depends on the amount of TM atoms. In the HAADF-STEM image in Fig. 2(a), the TM layers along the $[1\,1\,\bar{2}\,0]$ direction mainly have a pattern in which a pair of two bright columns (TM-rich columns) is followed by one dark column (Li-rich column). This result indicates that the regular arrangement of –TM–TM–Li– in the TM layers was directly observed in the Li-rich solid-solution layered cathode material $Li[Ni_{0.17}Li_{0.2}Co_{0.07}Mn_{0.56}]O_2$. The constant period is about three times as long as the $(1\,1\,\bar{2}\,0)$ spacing. This periodicity is clearly observed as the characteristic streaks indicated by the downward arrows in the SAED pattern in Fig. 2(a), which are located at the 1/3 and 2/3 positions between $\pm(1\,1\,\bar{2}\,l)$ and $(0\,0\,0\,l)$ (l: integer) diffraction spots formed from the primitive crystal system. This result is consistent with a $\sqrt{3} \times \sqrt{3}$ Li-ion ordering in the TM layers. For the sake of simplicity in this paper, we define this periodicity as *the three-times-periodicity*. It is noticed that the contrast intensities of the TM-rich columns and Li-rich columns in the TM layers changed in some TM layers, as Lei et al. reported for the $Li_{1.2}Ni_{0.2}Mn_{0.6}O_2$ ($Li[Ni_{0.2}Li_{0.2}Mn_{0.6}]O_2$) cathode material [11]. On the other hand, no periodic information was observed in the HAADF-STEM image and SAED pattern in Fig. 2(b), which were taken along the $[1\,1\,\bar{2}\,0]$ zone axis. Therefore, we will mainly discuss the structural changes with HAADF-STEM images along the $[1\,0\,\bar{1}\,0]$ zone axis.

Fig. 3(a) shows an atomic resolution HAADF-STEM image along the $[1\,0\,\bar{1}\,0]$ zone axis for the first fully charged $Li[Ni_{0.17}Li_{0.2}Co_{0.07}Mn_{0.56}]O_2$. As shown by comparison to Fig. 2(a), the three-times-periodicity disappeared. This result indicates that the Li ions in the TM layers participated in the charge process in addition to the Li ions in the Li layers. Regarding the participation of the Li ions in the TM layers in charging and discharging for this

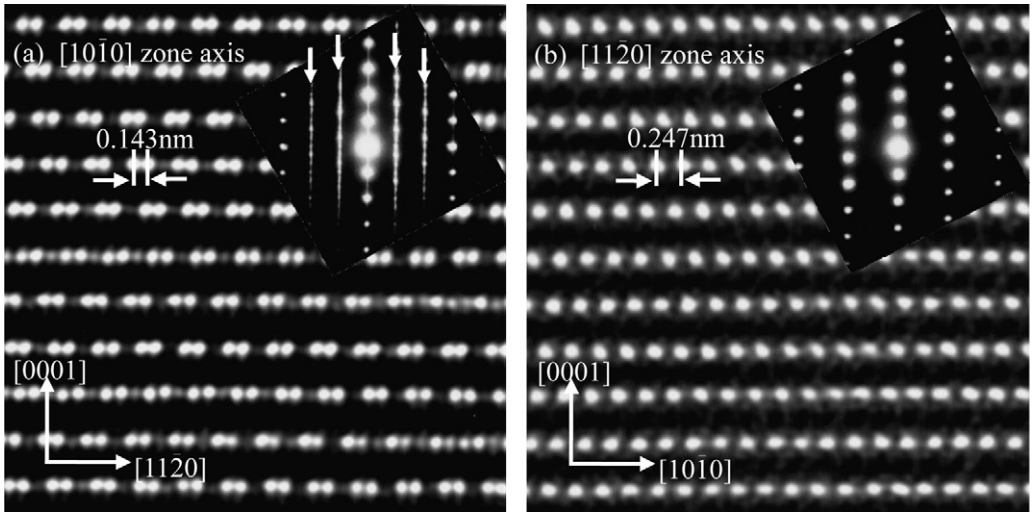

Fig. 2. Atomic resolution HAADF-STEM images for the as-prepared particles along the (a) $[1\,0\,\bar{1}\,0]$ and (b) $[1\,1\,\bar{2}\,0]$ zone axes. Insets in both images are the corresponding SAED patterns. In (a), the bright dots and dark dots in the TM layers in the HAADF-STEM image correspond to the TM-rich columns and the Li-rich columns, respectively. The streaks in the SAED pattern in (a), as designated by the downward arrows, are the result of the three-times-periodicity.

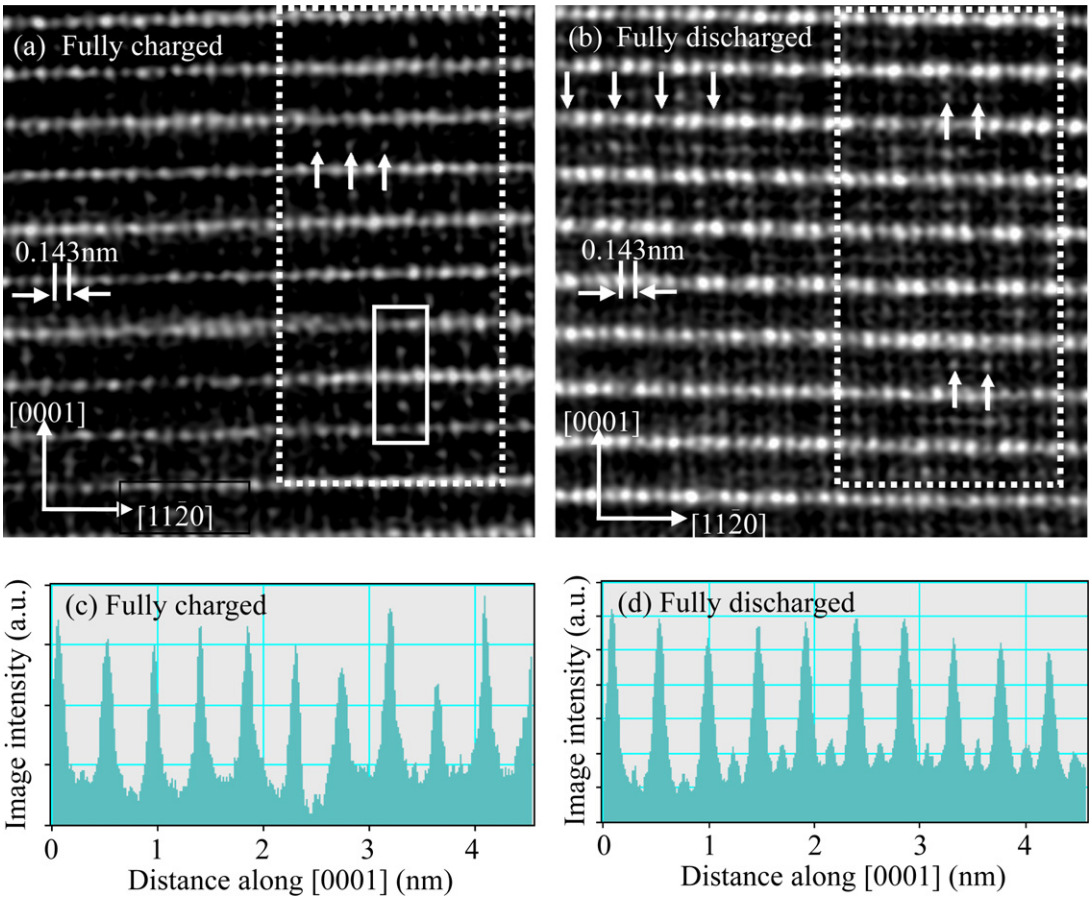

Fig. 3. Atomic resolution HAADF-STEM images for (a) the fully charged and (b) the fully discharged particles along the [1 0 $\bar{1}$ 0] zone axis. The upward and downward arrows indicate the two-times-periodicity and the three-times-periodicity, respectively. The rectangular region designated by the solid line in (a), which includes the two-times-periodicity, indicates a spinel structure, as discussed in Fig. 5. (c) and (d) are the image intensity profiles of the region designated by the dotted lines in (a) and (b), respectively, as a function of position along the [0 0 0 1] direction.

sort of materials, Kang et al. have reported irreversible extraction of the Li ions in the TM layers from the *ex situ* X-ray study for Li $[Li_{0.2}Ni_{0.2}Mn_{0.6}]O_2$ during charging at a positive potential higher than 4.5 V [12]. Grey et al. have further reported reversible extraction of the Li ions in the TM layers from the ^{6}Li MAS NMR study for Li $[Li_{(1-2x)/3}Mn_{(2-x)/3}Ni_x]O_2$ during charging and discharging [13]. In addition to the disappearance of the three-times-periodicity, an essential change happened in the Li layers. Bright dots appeared in the Li layers, indicating the existence of TM atoms in these layers. It is likely that TM atoms in the TM layers were transferred to the Li layers during the charge process. The bright dots were rather regularly arranged in some Li layers, where they were located at every other column, as indicated by the upward arrows in Fig. 3(a). We call this periodicity *the two-times-periodicity*. This result indicates that a kind of framework structure formed, and this framework structure appeared to be a spinel structure, as discussed in Fig. 5.

Fig. 3(b) shows a HAADF-STEM image along the [1 0 $\bar{1}$ 0] zone axis for the first fully discharged $Li[Ni_{0.17}Li_{0.2}Co_{0.07}Mn_{0.56}]O_2$. The three-times-periodicity in the TM layers appeared again in some TM layers, as indicated by the downward arrows in the image. This result indicates that Li ions were inserted into the TM layers as well as the Li layers. It is therefore suggested that the extraction and insertion of Li ions in the TM layers are responsible for the large capacity of $Li[Ni_{0.17}Li_{0.2}Co_{0.07}Mn_{0.56}]O_2$. The two-times-periodicity in the Li layers observed in the fully charged particles remained in a few Li layers, as indicated by the upward arrows in Fig. 3(b).

Li et al. have reported similar behavior to that observed in our study from the electron diffraction study for the layered O3 $Li[Ni_{0.5}Mn_{0.5}]O_2$ in which about 0.1 of Li ion per formula unit is present in TM layer and an equivalent amount of Ni^{2+} is present in Li layer [14]. In their case, the Ni migration from Li layer to TM layer was considered to be coupled to the reversible Li ion extraction from TM layer on charge and discharge. Therefore the reaction mechanism of the layered O3 $Li[Ni_{0.5}Mn_{0.5}]O_2$ appears to be different from that of our material since an amount of Ni^{2+} in Li layer of our material is much smaller than that of Li ion in TM layer, considering the result reported for Li $[Li_{0.2}Ni_{0.2}Mn_{0.6}]O_2$ [6].

Fig. 3(c) and (d) demonstrates the average image intensity profiles of the regions designated by dotted lines in Fig. 3(a) and (b), respectively, as a function of position along the [0 0 0 1] direction. The large peaks in these profiles correspond to the TM layers. Small peaks were observed at the positions of the Li layers for both of the fully charged (Fig. 3(c)) and the fully discharged (Fig. 3(d)) particles, which clearly indicated the presence of TM atoms in the Li layers. The ratio of the TM atoms in the Li layers to that of the TM layers was related to the image intensity ratio of the small peaks to the large peaks. We estimated the image intensity ratio as follows: a series of atomic models of $Li[Ni_{0.17}Li_{0.2}Co_{0.07}Mn_{0.56}]O_2$ were constructed, where Li atoms in the Li layers and TM atoms in the TM layers were partly substituted by TM atoms and Li atoms, respectively; the multislice simulation program (HREM Research Inc.) was used to calculate the HAADF-STEM images of the models; finally the image intensity ratio was estimated. By comparing the image inten-

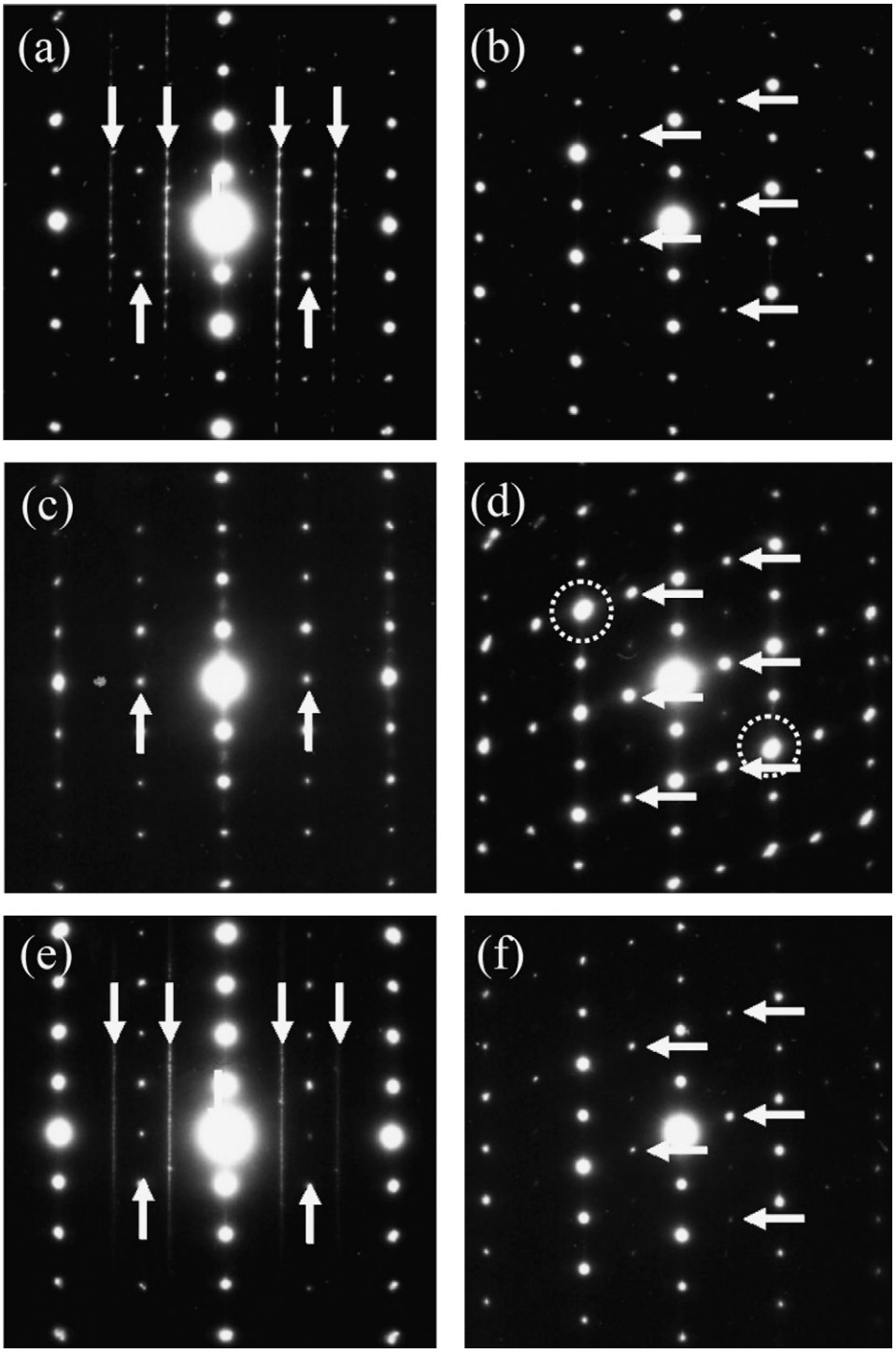

Fig. 4. SAED patterns (a) and (b), (c) and (d), and (e) and (f) for the first charge plateau region at 4.5 V, the fully charged state at 4.8 V, and the fully discharged state at 2.0 V as shown in Fig. 1, respectively. (a), (c) and (e) were taken from along the [1 0 $\bar{1}$ 0] zone axis, and (b), (d) and (f) were taken from along the [1 1 $\bar{2}$ 0] zone axis. The upward and downward arrows in (a), (c) and (e) indicate the two-times-periodicity and the three-times-periodicity, respectively. The satellites indicated by the horizontal arrows in (b), (d) and (f) were formed from the spinel structure and the twin-liked crystal structure that extends the area of the spots surrounded by the dashed circles, as detailed in Fig. 6.

sity ratio obtained from the average image intensity profiles with that obtained from the calculated image intensity, the quantities of the TM atoms at the Li layers and TM layers in Fig. 3(c) were estimated to be approximately 14 and 66%, respectively. Those at the Li layers and TM layers in Fig. 3(d) were estimated approximately 19 and 61%, respectively. It is clearly shown from the simulation results that many TM atoms were transferred from the TM layers to the Li layers during the charge and discharge processes.

To estimate the structural changes occurring during the charge and discharge processes, the SAED patterns along the [1 0 $\bar{1}$ 0] and [1 1 $\bar{2}$ 0] zone axes at stages 2, 3 and 4 in Fig. 1 are summarized in Fig. 4, among which stage 2 corresponds to the first charge plateau region at 4.5 V. In the SAED patterns along the [1 0 $\bar{1}$ 0] zone axis (Fig. 4(a), (c) and (e)), the streaks and the satellites designated by the downward and the upward arrows, respectively, correspond to the three-times-periodicity and the two-times-periodicity, as

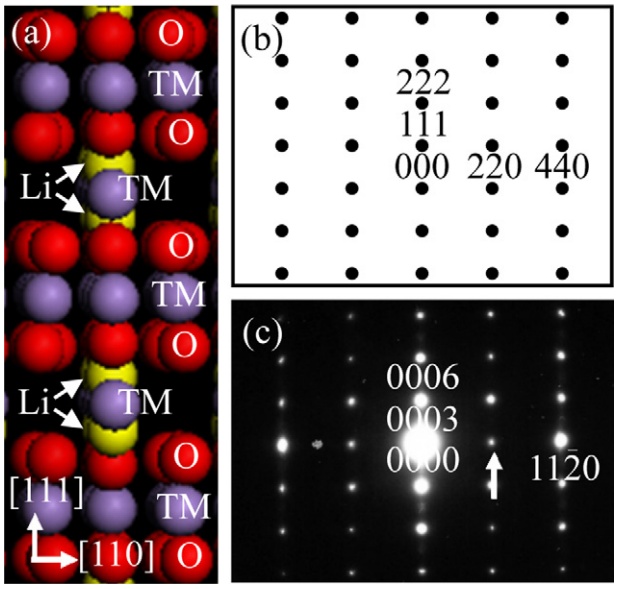

Fig. 5. Atomic model (a) of the spinel structure speculated from the rectangular region in Fig. 3(a) and the SAED pattern (b) calculated from the model along the [1 1 2] zone axis. (c) is equal to Fig. 4(c). The satellite designated by the arrow in (c) corresponds to the 2 2 0 diffraction spot in (b), which indicates the formation of a spinel structure.

discussed in Figs. 2(a) and 3. It is clear that the SAED patterns reflected the atomic arrangements observed in the atomic resolution HAADF-STEM images, although the measured area for the SAED patterns, which was a few hundred nanometers, significantly differed from that for the HAADF-images, which was only a few nanometers. This result indicates that the information from the HAADF-STEM images was nearly the same as that from the particles. The three-times-periodicity in the SAED patterns remained at the first charge plateau region at 4.5 V, and almost disappeared at the fully charged state at 4.8 V. The three-times-periodicity was observed again at the fully discharged state at 2.0 V. The two-times-periodicity was faintly observed at the first charge plateau region at 4.5 V, and clearly appeared at the fully charged and discharged states. The results indicate that the formation of the framework structural started at the same time as the electrochemical activation. Fig. 5(a) illustrates the atomic model of a spinel structure speculated from the rectangular region in Fig. 3(a), which has an fcc crystal structure [15]. Fig. 5(b) and (c) shows the SAED patterns calculated from the atomic model in Fig. 5(a) along the [1 1 2] zone axis and obtained from Fig. 4(c), respectively. The satellite designated by the arrow in Fig. 5(c) was nearly the same as the 2 2 0 diffraction spot in Fig. 5(b). Therefore, it is contemplated that the formation of the spinel structure was responsible for the appearance of the two-times-periodicity.

After the charge and discharge processes, the satellites appeared in the SAED patterns along the [1 1 $\bar{2}$ 0] zone axis, as designated by the horizontal arrows in Fig. 4(b), (d) and (f). These satellites were not observed for the as-prepared particles in Fig. 2(b). The satellites were assigned to the diffractions from the spinel structure along the [1 1 0] direction of the fcc structure. They were faintly observed at the first charge plateau region at 4.5 V and the fully discharged state at 2.0 V (Fig. 4(b) and (f)), indicating that a few spinel structures formed in the materials, which was consistent with the results obtained from the observation along the [1 0 $\bar{1}$ 0] zone axis. The satellites were clearly observed in the fully charged particles, as shown in Fig. 4(d), suggesting the promotion of the formation of the spinel structure. Furthermore, the area of the spots surrounded by the dashed circles was largely extended compared

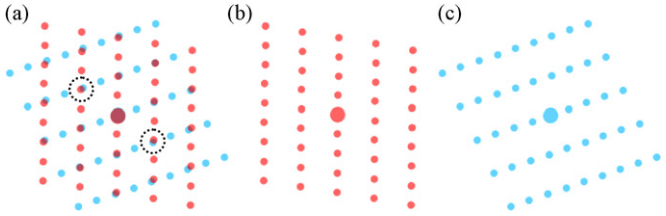

Fig. 6. Formation of the twin-like SAED pattern. The pattern in (a), as obtained from Fig. 4(d), consists of the two patterns of (b) and (c). The area of the spots surrounded by the dashed circles is largely extended compared with the other spots.

with the other spots. This heterogeneity was not explained only by the formation of the spinel structure. These extended spots are assumed to form not from a single crystal, but from more than two crystals. Fig. 6(a)–(c) shows the schematic patterns for the appearance of the satellites. Fig. 6(a), as obtained from Fig. 4(d), consisted of the two patterns of Fig. 6(b) and (c), where the two *c* axes were different from each other in the direction. Consequently, the spots surrounded by the dashed circles in Fig. 6(a) were extended in area. Although the relation between the two SAED patterns was not a twin structure in crystallography, it looked like a twin structure. Thus, we call it the twin-like structure. We confirm that the crystal structure deteriorated upon the initial charge and discharge and that this deterioration was especially promoted upon the initial charge, causing the partial formation of the spinel structure. To clarify the structural changes occurring after the cycle test, we are experimenting with the cycle test and will report the observed changes in the future.

4. Conclusions

Using atomic resolution HAADF-STEM and SAED, we have investigated the structural changes that occur during the first charge and discharge processes in a $Li[Ni_{0.17}Li_{0.2}Co_{0.07}Mn_{0.56}]O_2$ cathode material. HAADF-STEM directly detected the atomic arrangements of TM atoms, and the SAED patterns revealed the atomic arrangements and crystal defects. In the as-prepared $Li[Ni_{0.17}Li_{0.2}Co_{0.07}Mn_{0.56}]O_2$, a three-times-periodicity was present in the TM layers, as consistent with a $\sqrt{3} \times \sqrt{3}$ Li-ion ordering in the TM-planes. In the fully charged $Li[Ni_{0.17}Li_{0.2}Co_{0.07}Mn_{0.56}]O_2$, the three-times-periodicity almost disappeared after the transfer of some of the TM atoms in the TM layers to the Li layers, and a two-times-periodicity was clearly observed in many Li layers, showing the formation of a spinel structure. A twin-like structure was also observed, which led to the deterioration of the crystal structure. In the fully discharged $Li[Ni_{0.17}Li_{0.2}Co_{0.07}Mn_{0.56}]O_2$, the three-times-periodicity partly appeared again, and the two-times-periodicity still remained. At the early stage of the first charging in the plateau region around 4.5 V, the three-times-periodicity remained in the TM layers, and the two-times-periodicity was formed. This result indicates that the formation of framework structure started at the same time as the electrochemical activation. These structural changes mean that the structure was slightly different before and after the first cycle.

Acknowledgements

The authors would like to thank Dr. N. Endo of JEOL Ltd. for measuring the HAADF-STEM images. The authors acknowledge financial support from the Japanese New Energy and Industrial Technology Development Organization (NEDO) under the project "Development of High Performance Battery System for Next-Generation Vehicles" (Li-EAD project).

References

[1] K. Mizushima, P.C. Jones, P.J. Wiseman, J.B. Goodenough, Mater. Res. Bull. 15 (1980) 783.
[2] A. Ito, D. Li, Y. Sato, M. Arao, M. Watanabe, M. Hatano, H. Horie, Y. Ohsawa, J. Power Sources 195 (2010) 567, and references cited therein.
[3] Z. Lu, J.R. Dahn, J. Electrochem. Soc. 149 (2002) A815.
[4] Y.J. Park, M.G. Kim, Y.-S. Hong, X. Wu, K.S. Ryu, S.H. Chang, Solid State Commun. 127 (2003) 509.
[5] Y.-S. Hong, Y.J. Park, K.S. Ryu, S.H. Chang, M.G. Kim, J. Mater. Chem. 14 (2004) 1424.
[6] A.R. Armstrong, M. Holzapfel, P. Novák, C.S. Johnson, S.-H. Kang, M.M. Thackeray, P.G. Bruce, J. Am. Chem. Soc. 128 (2006) 8694.
[7] A. Ito, Y. Sato, T. Sanada, T. Ohwaki, M. Hatano, H. Horie, Y. Ohsawa, Electrochemistry 78 (2010) 380.
[8] A. Ito, Y. Sato, T. Sanada, M. Hatano, H. Horie, Y. Ohsawa, J. Power Sources, in press.
[9] A. Ito, D. Li, Y. Ohsawa, Y. Sato, J. Power Sources 183 (2008) 344.
[10] K. Ishizuka, Ultramicroscopy 90 (2002) 71.
[11] C.H. Lei, J. Bareño, J.G. Wen, I. Petrov, S.-H. Kang, D.P. Abraham, J. Power Sources 178 (2008) 422.
[12] S.-H. Kang, Y.-K. Sun, K. Amine, Electrochem. Solid-State Lett. 6 (2003) A183.
[13] C.P. Grey, W.S. Yoon, J. Reed, G. Ceder, Electrochem. Solid-State Lett. 7 (2004) A290.
[14] H.H. Li, N. Yabuuchi, Y.S. Meng, S. Kumar, J. Breger, C.P. Grey, Y. Shao-Horn, Chem. Mater. 19 (2007) 2551.
[15] J. Akimoto, Y. Takahashi, N. Kijima, Y. Gotoh, Solid State Ionics 172 (2004) 491.